Investigation of the long-term stability of quartzite and basalt for a potential use as filler materials for a molten-salt based thermocline storage concept

by Claudia Martin [a], Alexander Bonk [a], Markus Braun [a], Christian Odenthal [b], Thomas Bauer [b]

[a] German Aerospace Center (DLR), Institute of Technical Thermodynamics, Pfaffenwaldring 38-40, 70569 Stuttgart, Germany

[b] German Aerospace Center (DLR), Institute of Technical Thermodynamics, Linder Höhe, 51147 Köln, Germany

Keywords: basalt; quartzite; filler material; thermocline storage

Abstract

Solar thermal power plants with integrated thermal storage are candidates for renewable energy production concepts. For cost reduction of thermal energy storage a single tank concept, the so called thermocline storage concept, instead of the two-tank molten salt thermal storage is as promising cost reduction option. Further cost reductions in the thermocline storage are expected by replacing a significant amount of Solar Salt by a low cost filler material. Such filler materials have to be stable in molten salt at temperatures up to 560 °C. In this work degradation studies on quartzite and basalt types in molten salt are carried out after a preselection has been published elsewhere recently. The investigations are focused on the compatibility of natural stones with Solar Salt, a mixture of sodium nitrate and potassium nitrate, as common heat storage material.

This work addresses changes of the molten salt properties and in the microstructure of the natural stones depending on the exposure time in molten salt at temperatures of approximately 560 °C. In the first step of the material investigation the natural stones were isothermally stored in Solar Salt at a maximum temperature of 560 °C for up to 10.000 hours. After the thermal treatment the microstructure of the stones was investigated by QEMSCAN (Quantitative Evaluation of Minerals by Scanning electron microscopy). By means of this analysis method the changes in the microstructure of quartzite and basalt was detected and arising stone components are identified. The melting temperature und enthalpy of Solar Salt was measured and compared with the salt properties before the thermal treatment. Additionally, the specific heat capacities of basalt and quartzite depending on the temperature were determined. The results are essential to verify the suitability of quartzite and basalt as potential filler materials in modern thermocline storage concepts.

Published in; Solar Energy *171* (1) **2018**, 827-840

1. Introduction

1.1. Thermocline storage concept

Two-tank molten salt storage systems mark the current state-of-the-art for thermal energy storage (TES) in parabolic trough and solar tower power plants (Gil et al., 2010). In general, the two-tank storage system consists of two separate storage tanks, one operating at a higher temperature level (hot tank) and the other one at a lower level (cold tank). During charging, salt is extracted from the cold tank, heated to a higher temperature and subsequently stored inside the hot tank. The method of heating the salt distinguishes the two tank system into two concepts. In direct systems, the molten salt is directly heated inside the collectors of a parabolic trough power plant or inside the receiver of a tower power plant. Thus, molten salt and heat transferring fluid (HTF) in the plant are the same. In indirect systems, the HTF is different from the molten salt used in the storage system. A common example is the parabolic trough system with thermal oil, where the heat must be transferred from the oil to the salt through a heat exchanger.

To discharge the storage system, the charging process is reversed: In the direct system, molten salt can be extracted from the hot tank, fed into the steam generator and eventually stored inside the cold tank. In indirect systems an intermediate step is necessary, where the heat is first transferred to the HTF, which then transfers the heat to the steam generator.

One drawback of the two-tank concept is the poor utilization of the available volume of the tanks. For example, at the beginning of the storage process, the cold tank is filled with salt whereas the hot tank must be empty to store the hot molten salt. Hence, only 50 % of the available space is used.

The thermocline concept aims for further cost reductions in molten salt sensible heat thermal energy storage systems, by using only a single tank for storing molten salt (Libby, 2010). The working principle is illustrated in Figure 1 and differs from the two-tank system. To charge the thermocline storage, cold molten salt is extracted from the bottom of the tank and, after heating by the HTF, returned at a higher temperature level at the top of the tank. Due to the salt's lower density at higher temperatures, it remains stratified and does not mix with the colder salt. For discharging the process has to be reversed. With this technology, costs for foundation, tank material and piping of the cold molten salt tank can be reduced significantly (Libby, 2010).

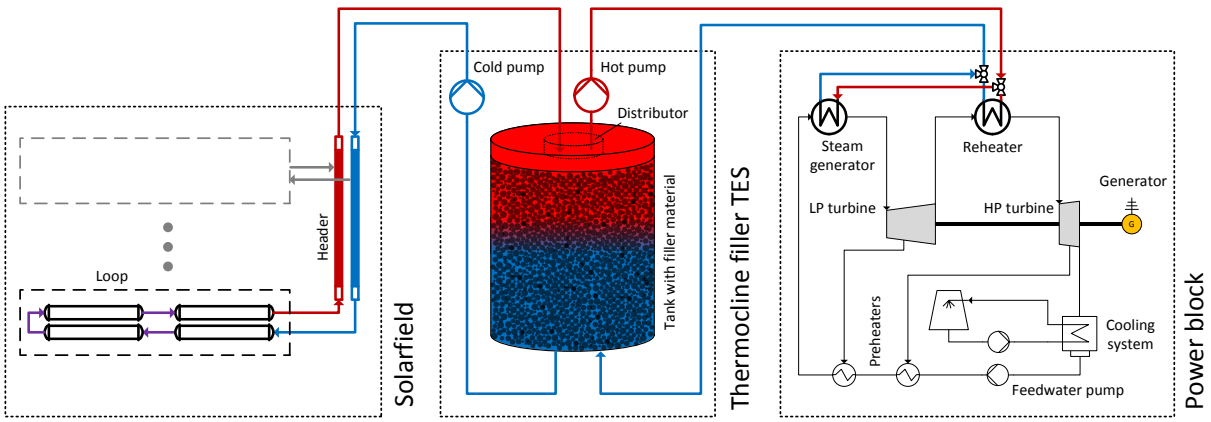

Figure 1 An illustration of the thermocline storage tank in a solar trough power plant.

A vast potential for further cost reduction is the use of cheap filler material. For this concept, a low cost filler material is embedded in the storage tank, replacing Solar Salt. Whilst at the

Published in; Solar Energy *171* (1) **2018**, 827-840

time of writing, costs for molten salt lie in the range of 500-1000 €/t, filler materials – such as basalt – are as low as 50 €/t and their volumetric heat capacity is comparable to that of molten salt (Martin et al., 2014) . Although utilization of these systems is a little lower due to limited heat transfer between filler and molten salt, the overall cost reduction potential can be up to 40 % (Libby, 2010).

The thermocline concept was first demonstrated by Sandia (Faas et al., 1986). The investigated thermocline storage was the largest system to date and part of the Solar One power plant with 170 MWh_{th} capacity. As filler material granite rock and as HTF thermal oil (Caloria HT-43) was used, which limited the operation temperature to 300 °C. Besides the storage system itself, chemical and mechanical stability have been investigated as well. The largest system using molten salt has also been built at Sandia (Pacheco et al., 2002). The authors presented results of a 2.3 MWh_{th} storage module with a maximum operation temperature of 400 °C. Another mid-sized thermocline system based on thermal oil with 350 °C temperature has been investigated at CEA (Bruch et al., 2014). Later CEA presented a 30 m^3 thermocline storage system, as part of a small ORC Fresnel power plant with an operating temperature of 300 °C. The storage system uses thermal oil and unclassified rock as filler material (Rodat et al., 2015). A smaller experiment with rapeseed oil/ quartzite rock and 8.3 kWh_{th} has been recently presented by PROMES-CNRS (Hoffmann et al., 2016). Gil et al. (2010) presented an overview of the research activities to the thermocline storage concept with one single tank for molten salt storage instead of two tanks.

At the DLR site in cologne, a thermocline test facility with 22 m^3 storage volume has been installed and is now in the commissioning phase (Odenthal et al., 2017). An illustration of the storage volume is shown in Figure 2. Each component is equipped with electric trace heating to minimize heat losses to the environment. This is particularly advantageous for the storage volume which can thus be considered adiabatic. Inside the storage volume 150 thermocouples measure the three-dimensional temperature field. The filler material is held by a stack of three removable baskets. Through this design, test arrangements can be prepared on the outside and later inserted into the storage tank. Hot and cold molten salt is provided by two reservoir tanks, whose temperatures can be individually adjusted. These reservoirs imitate the behavior of attached energy sources or sinks (i.e. heater, solar collector or power plant). The pumps are designed for a molten salt mass flow of more than 14 tons/h at 560 °C.

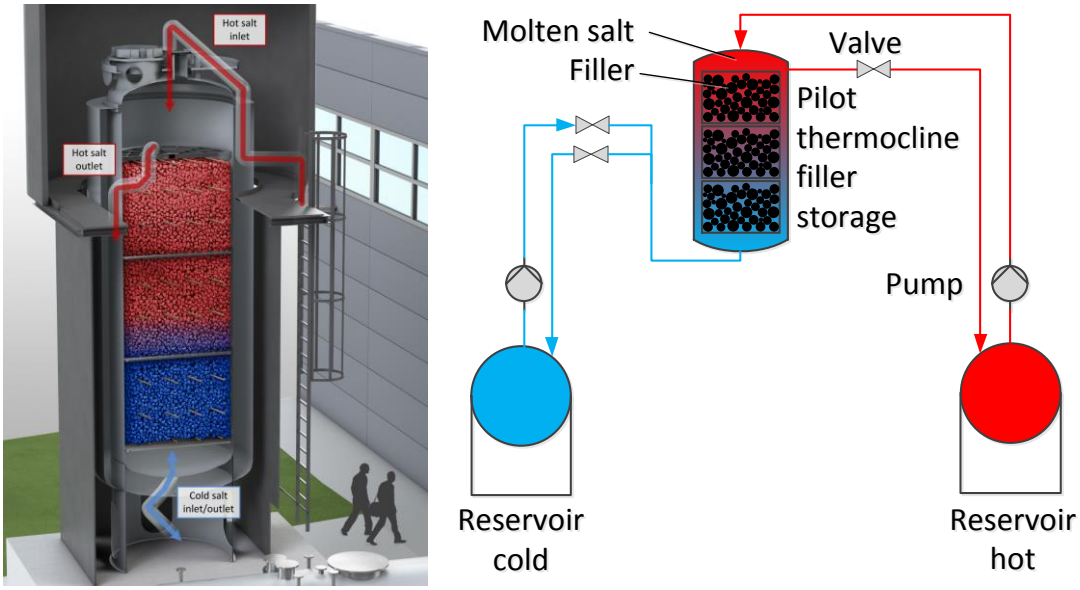

Published in; Solar Energy *171* (1) **2018**, 827-840

Figure 2 An illustration of the thermocline test facility (left) and the related P&I diagram (right).

The operation of the TESIS plant, and other thermocline systems in general, works as follows: During discharging, cold salt flows into the storage volume at the bottom and flows through the filler material up to the top, where it is extracted from a pipe attached on the side. Heat is transferred from the hot filler material to the initially colder molten salt. The heat transfer is usually limited to a region between already cooled and yet hot filler material, which is called the thermocline zone. This thermocline zone slowly moves through the storage volume until it reaches the top. At this point, the exit temperature of the hot salt will decline, having negative effects on the power unit attached to the storage system. Hence, a thin thermocline zone is favorable, keeping the exit temperature at a constant level for as long as possible. Previous publications dealing with the optimization of thermocline systems confirm that the operation strategy significantly affects the shape of the thermocline zone and eventually influences the thermal behavior of such thermocline systems (Bayón and Rojas, 2013).

Looking at recent theoretical publications, it can be noted that focus lies either on more specific effects or system simulations. One of the more specific topics is the effect of thermal ratcheting which has been addressed by CEA (Sassine et al., 2016), Sandia (Kolb et al., 2011), at Purdue University (Flueckiger et al., 2013) and ETSEIAT (González et al., 2015). The effect is caused by a thermally expanding storage vessel which might cause the packing to collapse. When the vessel is cooling down during discharging, its contraction is inhibited by the packing, causing mechanical strain. However, most publications could not find signs of ratcheting but state that at higher temperature different scenarios might occur.

Chang et al. (2016) investigated the impact of modifications of the inner tank walls on the thermal performance of thermocline storage tanks. Gaggioli et al. (2015) presented a molten salt storage system with an embedded heat exchanger for steam production. This embedded approach promises cost reductions and a better thermal stratification.

EPRI and Sandia carried out a comprehensive study, where the thermocline concept was compared to the two-tank system for various power plant design cases (Libby, 2010; Kolb et al., 2011). The study uses a power block in TRNSYS and a cost model to evaluate specific costs from annual simulations. At CIEMAT and the Cyprus Institute preliminary research has been conducted to model thermocline behavior with analytic functions (Bayón & Rojas, 2014; Votyakov & Bonanos, 2015). Later these models have been used to study operation strategies for solar thermal power plants with thermocline storage systems (Biencinto et al., 2014).

Overall, it can be seen that the molten salt thermocline filler concept is of high interest by several groups dealing with solar thermal energy storage. Among few other concepts like floating barrier and embedded heat exchanger, molten salt thermocline filler concept is currently seen as the major concept for cost reduction of two tank molten salt storage system.

1.2. Filler materials

In cost efficient thermocline storage tanks molten salt will be replaced by natural stones which have to be significantly cheaper than the used molten salt. The natural stones should have a high density, high mechanical strength and a sufficiently high specific heat capacity (Martin et al., 2014). The filler material must be available in large quantities at a low price level for a significant cost reduction, stable at high temperatures up to 560 °C and compatible with the selected molten salt. Natural stones which are used as raw materials for building

roads and rail tracks are suitable candidates. Filler materials with a high gross density and compressive strength are found in the group of sedimentary rock like quartzite and greywacke and also in the group of magmatic rocks which are often called hard rock due to their high compressive strength. Suitable magmatic rocks are for example diabas and basalt.
Natural stones were previously investigated as thermal storage material for high temperatures with air as heat transfer medium. A study of potential materials in a rock bed regenerator type thermal storage with air as HTF (100 thermal cycles from ambient temperatures up to 500 °C) showed that basalt, quartzite and granite are potential candidates for the use as thermal energy storage material (Riaz et al., 1977). For all of the investigated stones (basalt, granodiorite, quartzite, sandstone and limestone) cracking occurred mainly during the initial cycles. Basalt showed good mechanical properties because of its high compressive strength and tensile strength remained constant during the thermal tests.
Granite was already investigated regarding its compatibility to a binary and a ternary salt mixture at temperatures of 550 °C for 700 hours (Burolla and Bartel, 1979). The authors studied the stability of granite rocks and pelletized iron ore (taconite pellets) in a binary mixture (46 wt.-% sodium nitrate and 54 wt.-% potassium nitrate) at temperatures up to 550 °C. Granite rocks and taconite pellets kept in contact with the binary salt mixture, granite rocks were tested additionally in a ternary salt mixture (53 wt.-% potassium nitrate, 40 wt.-% sodium nitrite and 7 wt.-% sodium nitrate). The material analysis showed that granite is not a suitable filler material in salt mixture due to significant not-self-limiting erosion and dissolution processes. However, taconite was found to be compatible with the binary salt mixtures and can potentially be used as filler material.
Material studies concerning natural stones as filler material were presented by Pacheco et al. (2002) and Brosseau et al. (2005). Pacheco et al. (2002) presented the results of isothermal tests up to 1.000 h in Hitec XL® nitrate salt (43 wt.-% KNO_3, 42 wt.-% $Ca(NO_3)_2$ and 15 wt.-% $NaNO_3$) with a maximum temperature of 400 °C. The following natural stones have been tested: anhydrite, barite, bauxite, carborundum, casiterite, corundum, fluorapatite, hydroxyapatite, illmenite, limestone from Kansas and New Mexico, magnasite, marble, quartzite, scheelite, taconite and witherite. Additionally, a few natural rocks were tested in contact with a binary salt mixture (60 wt.-% sodium nitrate and 40 wt.-% potassium nitrate): limestone, marble, quartzite and taconite. Taconite, marble, limestone from New Mexico and quartzite were selected for thermal cycling test due to their availability, low costs and compatibility with molten salt. Potential filler materials are silica filter sand, quartzite and taconite because these natural rocks are compatible with nitrate salts. Quartzite and silica sand are the most practical filler materials due to their availability and low costs. Further tests regarding the thermal stability in nitrate salt and detailed investigations of the surface modification of the quartzite after thermal load were presented by (Brosseau et al., 2005). The thermal tests were performed with a ternary salt mixture (44 wt.-% potassium nitrate, 44 wt.-% calcium nitrate and 12 wt.-% sodium nitrate) as HTF and quartzite as filler material up to 500 °C and an exposure time of one year. The additional thermal cycling tests were conducted between 285 and 450 °C. A minimal deterioration of the tested filler material was observed during the thermal tests with a maximum duration of one year. However, there are concerns about the use of quartzite as filler material in combination with Ca-rich molten salt in commercial-scale power plants due to the formation of a significant $CaCO_3$ crust consisting of calcite, calcium carbonate and dicalcium silicate (Brosseau et al., 2005).
Material investigations of five natural stones (quartzite, basalt, granite, hornfels and marble) were also conducted by Grirate et al. (2014) for a thermal oil direct thermocline storage

system. The porosity, the thermal stability up to 400 °C and the specific heat capacity at 300 °C for the selected stones were determined. Basalt and quartzite had a good thermal stability, adequate specific heat capacity and comparable values for porosity and density. Eventually, the quartzite was chosen as the best filler material after the presence of mafic minerals in basalt was found non-beneficial. The authors presented concerns that the mafic minerals contaminate the thermal oil. The study was pursued and extended to an additional natural stone: cipolin. The stone was characterized for its use in the direct contact with synthetic oil in a thermocline storage concept in the temperature range 250 to 350 °C. Material properties up to 300 °C and thermal stability up to 400 °C are presented and summarized by Grirate et al. (2016). Quartzite and cipolin are chosen as potential filler materials.

In technical review studies, as presented by Gil et al. (2010), quartzite and silica sand is recommended as suitable low price filler material, so that it is promoted for a lot of theoretical investigation. Besides the investigations of natural rocks as potential filler materials, several studies considered industrial waste products as potential sensible storage materials. One potential candidate of the group of industrial waste materials is examined by Calvet et al. (2013). The promising filler material is a post-industrial ceramic and called Cofalit®. The thermal stability of Cofalit® was tested in two molten salts with a maximum temperature of 500 °C for 500 h: the binary salt mixture Solar Salt and a ternary Hitec XL. The surface and internal structure of the samples were investigated after the thermal treatment in the molten salt mixtures. The results show that Cofalit® has the potential to be used as filler material in Solar Salt. The study of Ortega-Fernández et al. (2015) focused on the use of steel slags as sensible storage material. The main components of the analyzed slags were iron oxide, calcium oxide and silicon oxide. Several material investigations were performed for characterization on the new potential storage material. Thermal stability was measured in an air atmosphere up to 1.100 °C. The mass loss is negligible and the slags were considered stable up to 1.100 °C. However, isothermal storage of the stone structure and subsequent analysis after 24 h at 1.000 °C has shown that changes in the slag structure are possible and phases with a higher oxidation rate may form. A comparison with another potential sensible storage material presented by Ortega-Fernández et al. (2015) demonstrated a high storage density of the cheap steel slags and has shown a high potential as sensible storage material. The thermal stability in a molten salt mixture was not investigated.

Beside natural stones, other buildings materials are investigated as potential filler materials. John et al. (2013) investigated various concrete mixtures as thermal storage material also for their use in molten salt. After the thermal treatment the compressive strength was found to be reduced significantly. Magnetite with a high content of iron oxide (over 90 % Fe_2O_3) was tested by Grosu et al. (2017) regarding thermal stability (up to 1.000 °C) in air atmosphere. The use in a thermocline storage unit with molten salt was not considered. Focus of the investigation was the determination of material properties such as density, compressive stress, thermal conductivity, thermal diffusivity, and antiferromagnetic transition. Thermally treated magnetite was identified as a suitable sensible storage material with adequate thermophysical properties in air atmosphere.

Previous investigations including those of the presenting authors have shown that natural stones are potential filler material whereby quartzite and basalt are the most promising candidates from the group of natural stones. Preliminary tests for thermal stability up to 900 °C were done. Cyclic and isothermal tests with a maximum duration of 1.000 hours with a maximum temperature up to 560 °C were performed.

Overall it can be stated that studies of natural stones in thermocline concepts are diverse and hardly comparable since different natural stone types and heat transfer fluids were used. It is reasonable to assume that the intended CSP type and storage process is one of the main drivers for the research activities. Additionally the highly relevant economic aspect requires for the investigation of locally available natural stones, since transportation is one of the largest contributors to the final price of the filler material.
This paper presents recent work on the material aspects and stability of selected filler materials for operation temperatures up to 560 °C in Solar Salt, which is state-of-the-art in modern CSP plants. Especially the high temperature of 560 °C combined with long exposure time up to 10.000 h and extensive subsequent material analysis by QEMSCAN make this work unique in the field of CSP-TES material studies and provide an in-depth view on the stability of the most promising filler candidates under relevant conditions. The knowledge about the changes in the microstructure should help to verify the potential of the selected filler candidates under technically relevant conditions.

1.3. Specification of basalt and quartzite

In previous studies (Martin et al., 2014) basalt and quartzite were selected as potential inexpensive filler materials. Depending on the mining area the basalt composition varied, so that two different basalt varieties were tested: the basalt from the mining area *Rossdorf* (abbreviation in that study BaRo) and from the mining area *Huehnerberg* (abbreviation in that study BaHu). Relevant thermal and physical properties of the natural stones are presented in Table 1 and Table 2.

Table 1 Selected material properties for selected natural stones DIN 52100-2:2007-06 (DIN Deutsches Institut für Normung e.V., 2007)

	Selected natural stones		
Material properties [unit]	**quartzite**	**basalt**	**reference**
Gross density [kg/m³]	2450-2700	2500-3100	DIN 52100-2:2007-06
Compressive strength [N/mm²]	150-250	150-300	DIN 52100-2:2007-06
Flexural strength [N/mm²]	11-25	13-25	DIN 52100-2:2007-06

Table 2 Specific heat capacities of quartzite and basalt measured in previous investigations (Martin et al., 2014)

	Specific heat capacity at various temperatures [kJ kg^{-1} K^{-1}]			
Filler type	**300 °C**	**400 °C**	**500 °C**	**560 °C**
Quartzite	1.052	1.103	1.144	1.29
Basalt BaHu	0.897	0.914	0.917	0.916

The material properties of quartzite and basalt like gross density, compressive strength and flexural strength are in the same range. The measured specific heat capacity of quartzite is higher than for basalt (Martin et al., 2014). Previous investigations of the thermal stability up to 900 °C were performed by TG-MS (thermogravimetric coupled with mass spectrometry) analysis in an air atmosphere. The mass loss of quartzite was negligible. In contrast, basalt displayed a mass loss of about 2 wt.-% in the first measurement cycle, while it was negligible in the second cycle. Overall, the mass loss was ascribed to reaction on the surface of the

basalt particles and small amounts of calcite in the sample. The calcite content of basalt and quartzite is negligible because there was no reaction in contact with hydrochloric acid as shown in a recent study (Martin et al., 2014).
Quartzite and basalt vary widely in their composition. Quartzite mainly consists of silica (SiO_2) with a share of 99 wt.-%. Other components of quartzite are alumina (Al_2O_3) and small amounts of iron oxide (Fe_2O_3), titanium oxide (TiO_2), potassium oxide (K_2O), sodium oxide (Na_2O), calcium oxide (CaO) and magnesium oxide (MgO) (Fa. Dorfner GmbH, 2012). In contrast to quartzite, basalt has a variety of components. Basalt is the most common volcanic rock with a high availability, high density and strength. A distinction is made between basalt in the strict sense and basalt in a broader sense. The composition of basalt varied depending on the strip mining area. The basalt BaHu mainly consists of clinopyroxene, plagioclase, olivine and layered silicates. The main components of the basalt BaRo are clinopyroxene, nepheline and also layered silicates. The shape of the particles is also different (In this paper, the term particle stands for a single stone in the loose filling). As shown in Figure 3, the quartzite particles have rounded edges while basalt particles are angular.

Figure 3 Particles *of quartzite (left), basalt mining area Huehnerberg (middle) and basalt mining area Rossdorf (right)*

Quartzite shows a special feature, the so called quartz inversion, at a temperature of 573 °C (Smykatz-Kloss, 1970). The quartz inversion is a change of the crystal structure from β-quartz, with a trigonal structural type, to α-quartz, with hexagonal structural type. The change is reversible, endothermic and associated with a volume change in the range of between 1 and 1.4 % (β → α). The heat of transformation is 5.9 kJ kg^{-1} (Bazant and Kaplan, 1996). The quartz inversion is obviously detected in the measurement signal of the differential scanning calorimeter (DSC). The costs for the natural stones are overall in the same range with around 50 € per ton. The effective cost of one ton natural stone mainly depends on the specific transport route from the strip mining to the thermal storage unit. Therefore, stone-molten salt combinations must be chosen according to the desired power plant destination if cost reduction is the major goal.
The focus of this paper is the detailed specification of the stones composition before and after the thermal treatment in Solar Salt by using QEMSCAN analysis. The investigations show detailed that the components of the microstructure are changed and which components decrease and increases. Together with the results of the salt analysis, it should provide further indication which filler material is more suitable.

2. Experimental methods

2.1. Measurements of the specific heat capacity

Measurements of the specific heat capacity by using a differential scanning calorimeter (DSC, Netzsch DSC 204 *F1 Phoenix*®) were repeated at least five times for each filler material. The specific heat capacity of quartzite and basalt (strip mining *Hühnerberg*) are determined using a heating rate of 10 K/min in an argon atmosphere and within a temperature range from 40 up to 600 °C. The measurements of the specific heat are performed in accordance with DIN 51007 & ASTM E1269-11 and DIN 51007.

2.2. Thermal treatment of the natural stones and analysis of the stone structure afterwards

The focus of the investigations is the structural changes of natural stones in Solar Salt at high temperatures. Solar Salt is a nitrate salt mixture consisting of 60 wt.-% sodium nitrate ($NaNO_3$, Merck, analytical grade, >99%) and 40 wt.-% potassium nitrate (KNO_3, Merck, analytical grade, >99%) with a minimum melting temperature of 222 °C. The thermal cyclic tests are done in a conventional laboratory oven (Nabertherm GmbH). Temperature cycles are carried out between 290 and 560 °C for 100 times with isotherms at 560 °C for 120 min, and 180 min at 290 °C with heating and cooling rates of 5 K/min. More detailed experimental procedures are described elsewhere (Martin et al., 2014). The isothermal tests were carried out in laboratory ovens (Nabertherm GmbH) with durations of 1.000, 2.000, 5.000 und 10.000 h. The natural stones are stored together with Solar Salt in aluminum oxide crucibles which were located in a ceramic tube filled with ceramic balls. Additionally, for each fillers two blank samples were isothermally stored under identical conditions: a blank filler sample without Solar Salt and blank Solar Salt sample without filler sample.
The realization of the thermal cyclic and isothermal test with a duration from 500 and 1.000 h was described in (Martin et al., 2014). The isothermal test with duration of 2.000 and 5.000 h were performed in the same experimental way. The thermal tests up to 10.000 h were realized in a modified laboratory oven as shown in Figure 4 in order to avoid salt creeping.

Figure 4 ***Modified oven with nine aluminum oxide crucible for isothermal long time tests with a duration of 10000 h***

Published in; Solar Energy *171* (1) **2018**, 827-840

The modified laboratory oven should prevent salt creeping of Solar Salt during the thermal tests. The upper part of the aluminum oxide crucibles was placed outside the oven so that, eventually, creeping salt solidified before leaving the crucibles. Also the height of the crucible was changed from 70 mm in the 5.000 h experiments to 280 mm in the 10.000 h experiments. The realized modifications were successful and the salt creeping was reduced significantly. The mass loss was detected to verify the dimension of salt creeping.
The natural stones selected before and after each isothermal storage were embedded in araldite resin which was cured 100 °C. A grind section was produced by a water-free abrasive fluid, to avoid dissolution of salt or reaction product in water, using classical grinding and polishing techniques. The microstructure of the sample material was analyzed by "Quantitative Evaluation of Minerals by Scanning Electron Microscopy", referred to as QEMSCAN analysis (QEMSCAN FEI Quanta 650 F, Thermo Fischer). After scanning the sample a software package (iDiscover Suite) is used for data evaluation and automatic mineralogical phase analysis. The combination of information of identified mineral phases and chemical phase characterization result in a quantitative mineralogical phase analysis with overview scans with an increment of 9.89 µm and details scan with an increment of 1.83 µm. The analysis of the particle sections by QEMSCAN gives information about the distribution and orientation of mineral phases before and after the thermal treatment as well as the changes in texture of the samples.

2.3. Analysis of Solar Salt after thermal treatment

The measurement of the melting point and melting enthalpy of Solar Salt were performed in two different differential scanning calorimeters depending on the intended temperature range (DSC 404 and DSC 204 (described earlier in section 2.1.) by Netzsch GmbH). The heating rate for the measurement of the melting point was 10 K/min and measuring temperature range from 40 °C up to 350 °C in an air atmosphere. Also, the melting enthalpy was determined also by differential scanning calorimetry (heating rate of 5 K/min, temperature range from 40 °C up to 600 °C). The thermophysical properties of the Solar Salt were measured before and after the thermal treatment. A small amount (20 mg) of the solidified salt was analyzed.
Ion chromotography (IC, Metrohm model 930 Compact IC Flex, Metrohm (Switzerland)) was used to investigate the composition of the salt before and after the thermal treatment. The chromatography column is a Metrosep A Supp analytical column (5 x 250mm) and a sample loop of 20µl. The used eluent (3.2mM Na_2CO_3 and 1.0mM $NaHCO_3$) was mixed by analytical grade sodium carbonate (0.5M, Titrinorm, VWR, Germany) and sodium hydrogen carbonate (0.5M, VWR, Germany). Calibration in the relevant concentration range was carried out by preparing and measuring standard solutions from Certipur® multi-ion standards (Certipur®, 1000mg/l ICP mutli-element standard, Merck). A square fit function through at least four concentrations was used and regression functions with $R^2 > 0.9999$ were accepted for analysis only.
Titration was carried to detect species of carbonates and dissolved oxide ions by using a Brand Titrette ® class. As titrant Merck Titrisol ® 0,01mol/L or 0,1mol/L, dependent on the expected oxide level in the sample, was diluted in 1L of deionized Water and a control titration was measured with analytical grade sodium carbonate. The used analysis method for measuring the salt composition is described more detailed by Bonk et al. (2017).

3. Results of the material investigations

3.1. Specific heat capacity of quartzite and basalt

The DSC measurements were performed to verify previous investigations of the specific heat capacity and obtain more statistically relevant values by increasing the number of measurements. The average value of a minimum of 8 individual measurements of the heat capacity of quartzite and basalt are shown in the following Table 3.

Table 3 Overview of specific heat capacities of quartzite and basalt measured in the DSC including previous investigations (Martin et al., 2014)

	Specific heat capacity at various temperatures [kJ kg^{-1} K^{-1}] (standard derivation)			
Filler type	**300 °C**	**400 °C**	**500 °C**	**560 °C**
Quartzite	1.077 (0.046)	1.139 (0.036)	1.217 (0.031)	1.377 (0.030)
Basalt BaHu	0.981 (0.072)	1.031 (0.079)	1.054 (0.091)	1.075 (0.097)
Basalt BaRo	1.051 (0.064)	1.087 (0.066)	1.107 (0.059)	1.120 (0.05)

The specific heat capacities of the basalt are smaller than for the quartzite and nearly constant over the measured temperature range. The specific heat capacity of quartzite is slightly increasing with temperature. The rise is caused by the quartz inversion at 573 °C described earlier. The specific heat capacity increased steadily with increasing temperature before the quartz inversion, as shown in Figure 5.

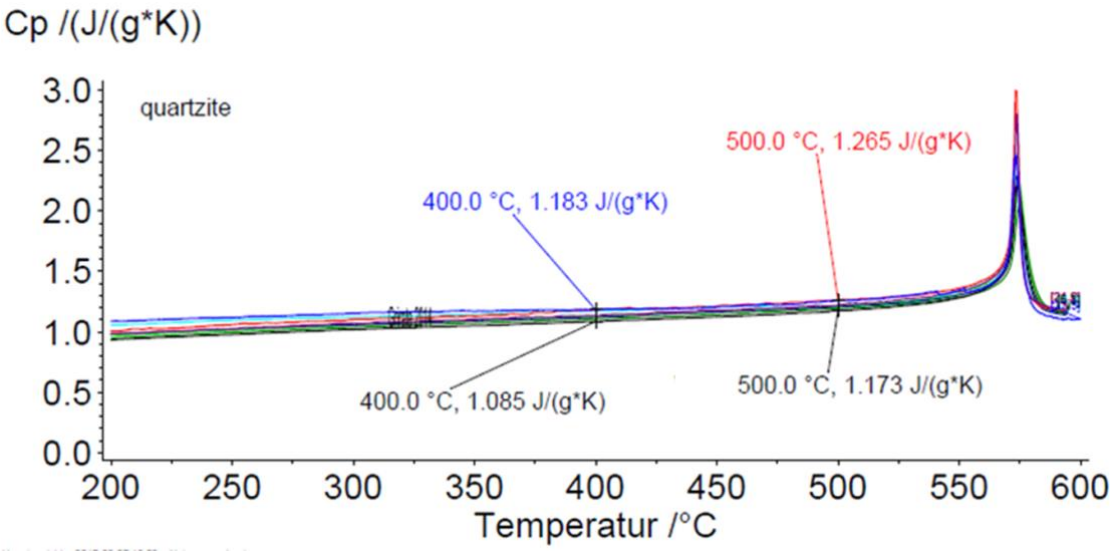

Figure 5 ***All measurement curves of specific heat capacity of quartzite (DSC, heating rate: 10 K/min, 40-600 °C, argon atmosphere, second measurement cycle).***

The DSC measurements in the DSC 204 confirm the result of the previous measurement in the DSC 404 (Martin et al., 2014). At a temperature of 300 °C the specific heat capacity of quartzite is similar to that of basalt, but with increasing temperature the specific heat capacity of quartzite is higher. Above 400 °C, the specific heat capacity of quartzite is higher than for

Published in; Solar Energy *171* (1) **2018**, 827-840

basalt. The gap between the specific heat capacity of basalt and quartzite becomes larger with the temperature because the heat capacity of the basalt varieties is steadily in contrast to the quartzite.
Summarizing the material properties of quartzite and basalt, it can be noted that quartzite mainly consisting of silica leading to quartz inversion at 573 °C. The specific heat capacity of quartzite is higher than for basalt especially in the temperature range above 400 °C. The quartz inversion is reversible and associated with a small volume change but there is no further information on the influence of the quartz inversion on the mechanical stability of quartzite. Basalt consists of a variety of minerals which can vary in their amounts. In contrast to the higher specific heat capacity of quartzite, basalt has a higher maximum values for gross density and compressive strength. Both properties are important for potential filler materials whereby the specific heat capacity determined the storage capacity if the storage unit.

3.2. Stone structure of the filler after thermal treatment

The mass loss of the stone samples without Solar Salt provides information about potential decomposition processes occurring under exclusively thermal treatment in air. The weight of the natural stones during thermal treatment at 560°C was detected up to a maximum duration of 5.000 h. Measurable mass losses were detected. For longer thermal treatment of natural stones up to 10.000 h no values are determined due to the limited oven capacities.
The two basalt varieties retain their color during all experiments. The quartzite particles however, show a color change from gray to rose as shown in Figure 6 after a heat treatment at 560 °C for 1.000 hours or more.

Figure 6 ***Change of color of quartzite during the thermal tests (left: before thermal treatment, right after thermal treatment).***

The color change of the quartzite particles is already detected after only a few hours of thermal treatment. It is suspected that the color change is caused by a phase transition of iron oxide impurities, more precisely from magnetite (Fe_3O_4) to hematite (α-Fe_2O_3). Above 300 °C, the α-Fe_2O_3 modification changes its color into matt red due weathering. (Cornell and Schwertmann, 2003)
The microstructure of the stones (mineral phase and its change after thermal treatment) was investigated using QEMSCAN analysis. The various components in the particles before and after the thermal treatment can be determined with this analysis method allowing for the detection of the most common conversion processes. In this section, the components of the microstructure of the natural stone particles before and after the thermal treatment are

described. In Figure 7 the components with the corresponding coloring, which are important for the following explanation, are presented.

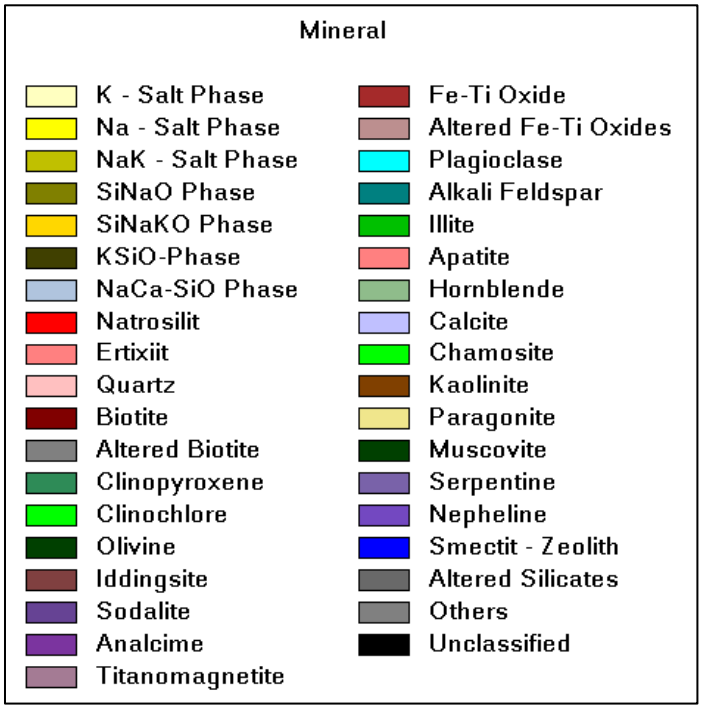

Figure 7 Color assignments used for the graphical representation of the QEMSCAN images.

First the natural stones structure before and after the thermal treatment without Solar Salt are presented. The investigated natural stones are exposed a thermal treatment of 560 °C for 2.000 h.

As shown in Figure 8, the microstructure of quartzite without Solar Salt due to the thermal treatment is unaltered. The light pink areas presented the original quartzite structure. In Figure 8(a) the particle structure without the thermal treatment and in (b) the microstructure after 2.000 h at 560 °C in air atmosphere is shown. There are no significant changes in the microstructure. The maximum temperature of the thermal treatment (560 °C) is slightly below the temperature of the quartz inversion (573 °C), so that transformation from α-SiO_2 to β-SiO_2 does not take place.

Published in; Solar Energy *171* (1) **2018**, 827-840

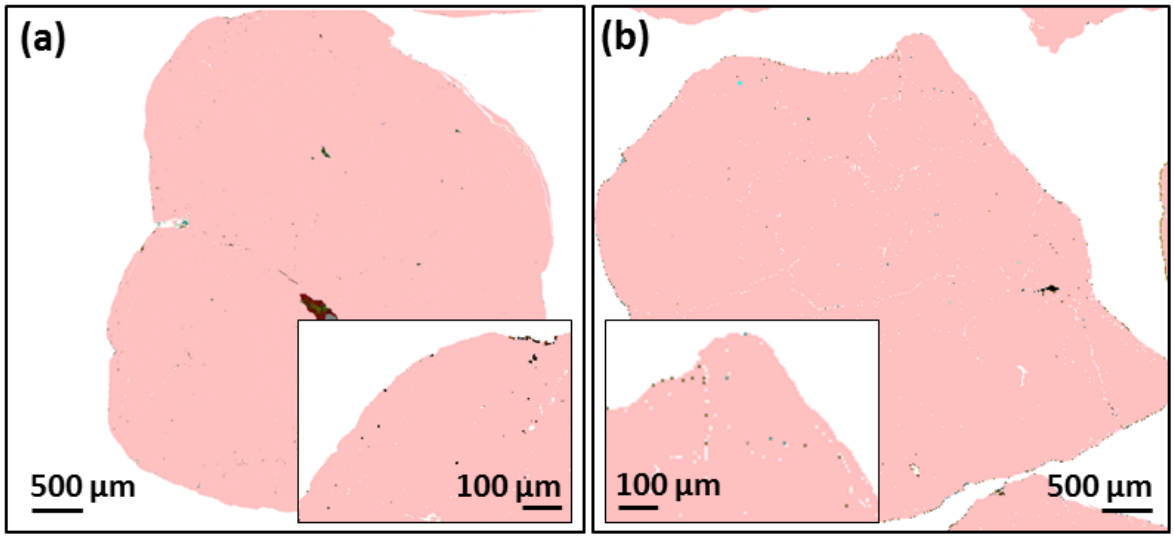

Figure 8 QEMSCAN images of quartz particles (a) before, and (b) after isothermal storage in air at 560°C. Inlets present a zoom into the particle-air interface of the respective sample.

Figure 9 and Figure 10 show the microstructure of the basalt varieties before and after the thermal treatment in an air atmosphere. First, the results for the basalt BaRo from the mining area Rossdorf are presented in Figure 9, nepheline in purple color and smectit-zeolith as dark blue colored area. Due to the similar size and distribution within the stone grain, nepheline ($NaAlSiO_4$) and smectit-zeolith, also consisting of sodium, aluminum, silicium and oxygen, it was assumed that the nepheline is transformed mainly into smectit-zeolith. Cracking is not observed, so that it is assumed that the transformation had no obvious influence on the stone structure.

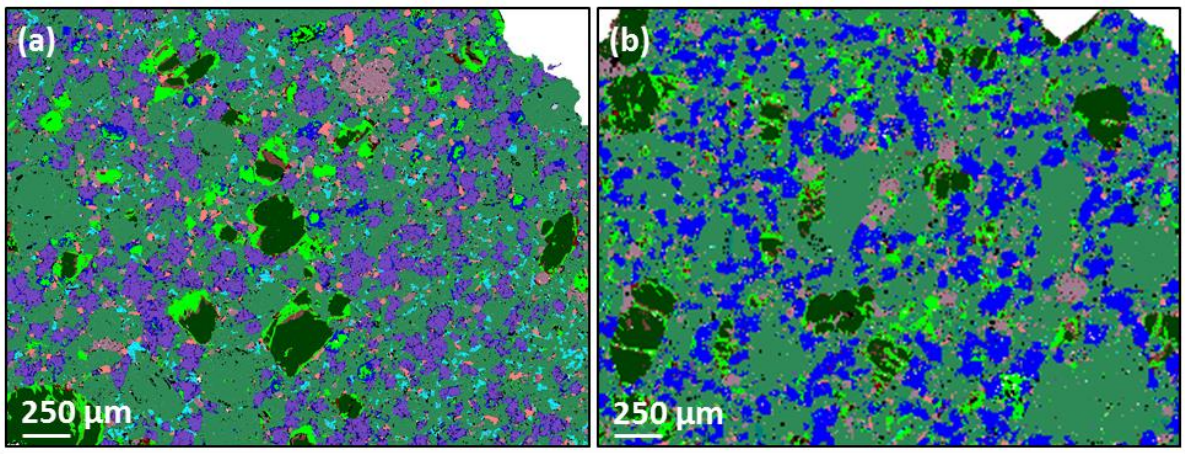

Figure 9 QEMSCAN image of BaRo (a) before and (b) after isothermal storage for 2.000h in air at 560°C.

After the thermal treatment of BaHu, as presented in Figure 10, the quantity of clinopyroxene in the microstructure of the investigated particles (dark green areas in Figure 10) decreases and the quantity of layered silicates (turquoise areas in Figure 10) increases. Cracking was not observed. So, it can be assumed that the transformation from a chain silicate to a layered silicate structure didn't lead to structural changes.

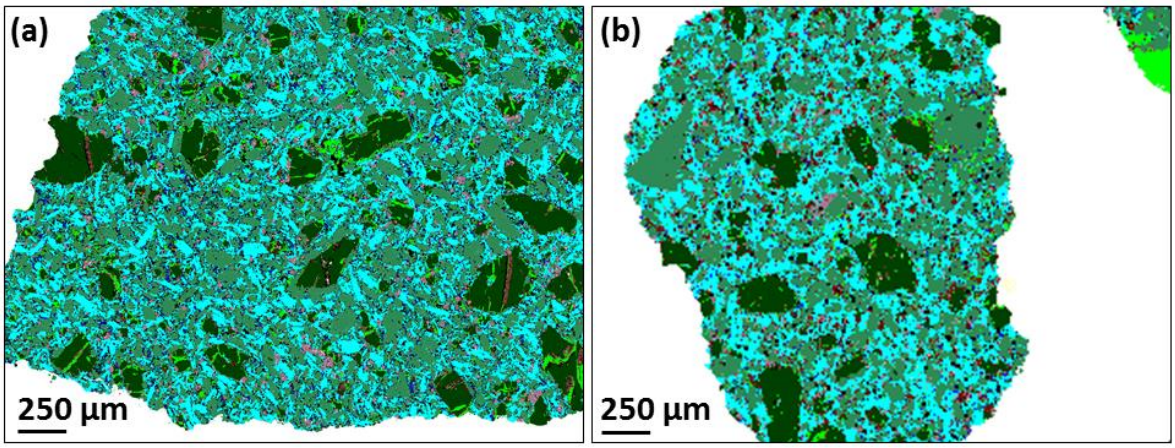

Figure 10 QEMSCAN image of BaHu (a) before and (b) after isothermal storage for 2.000 h in air at 560 °C.

The focus of the isothermal test was the thermal treatment of the selected natural stones together with Solar Salt. The maximum duration of the isothermal test was 10.000 h. First the results for quartzite are presented in the Figure 11.

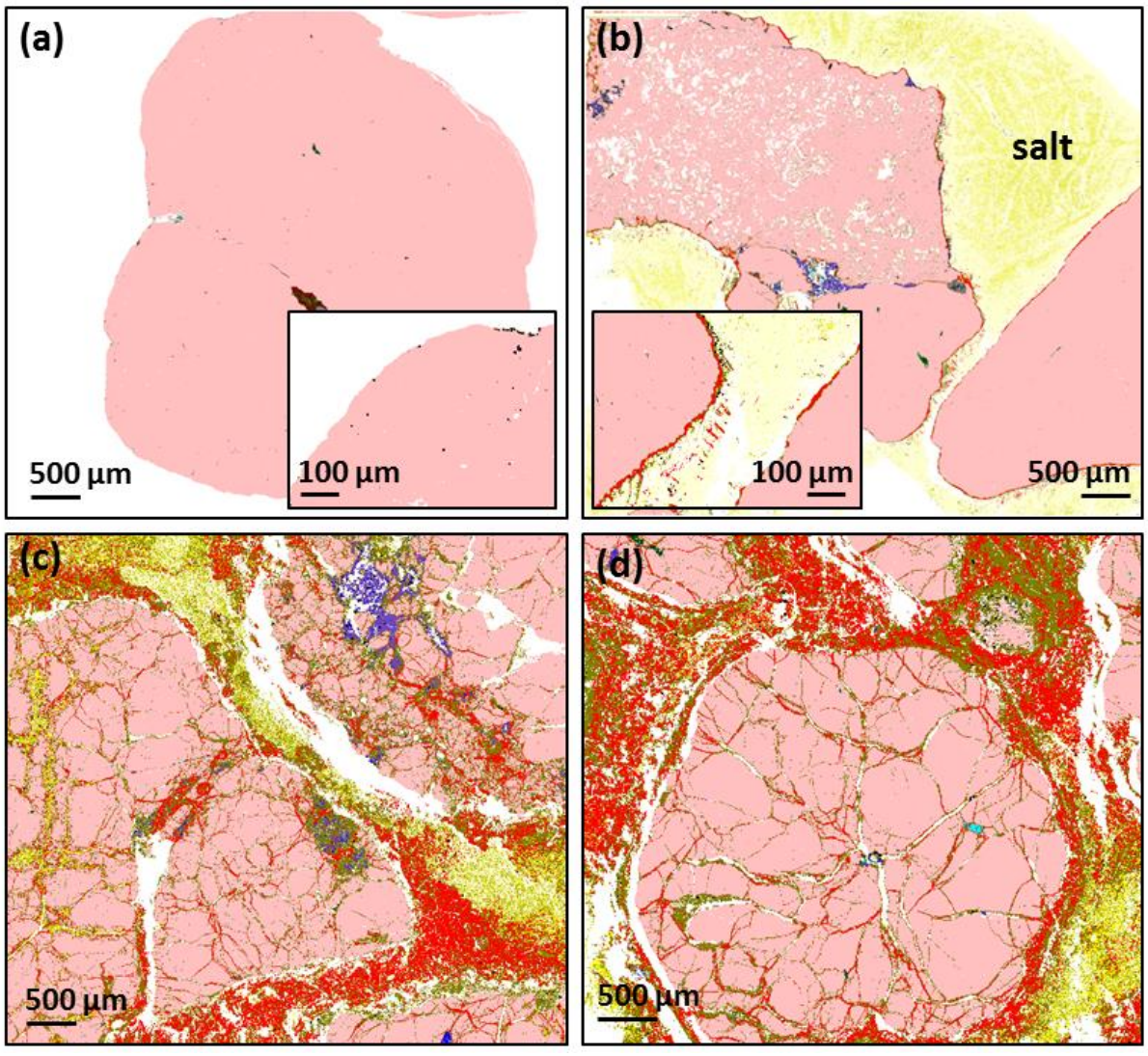

Figure 11 QEMSCAN images of quartz particle(s) (a) prior to the experiments and (b) after 1.000h, (c) 5.000h, and (d) 10.000h of isothermal storage in Solar Salt. Inlets in image (a) and (b) present zooms into the particle-air and particle-salt interface, respectively.

Published in; Solar Energy *171* (1) **2018**, 827-840

At the interface between particles and molten salt, natrosilit is formed. The structural formula of natrosilit is $Na_2Si_2O_5$ and is indicated by the red areas in Figure 11. Natrosilit can already detected after 1.000 h of thermal treatment, as shown in Figure 11 b. Natrosilit is a transformation product of sodium nitrate in the molten salt reacting with silica (SiO_2) as showed in equation (1).

$$SiO_2 + Na^+ \xrightarrow{transformation} Natrosilit\ (Na_2Si_2O_5) \quad (1)$$

Natrosilit has a high melting temperature of nearly 780 °C (Williamson and Glasser, 1965), so that it can be assumed that the natrosilit phase is solid at the operating temperature of 560 °C. Additionally, the amount of the SiNaO phase increase. The SiNaO phase is presented by the olive green areas in Figure 11. After 1.000 h, the SiNaO phase is located mainly in the outer pores and cracks as shown in Figure 11 b. With increasing duration of the thermal treatment the transformation to natrosilit and SiNaO phase is also inside the quartzite particles. The particle structure after 5.000 h and 10.000 h at 560 °C shows numerous cracks which are filled by natrosilit and SiNaO phase (Figure 11 c-d). Also, at the particle-molten salt interfaces the amount of both transformation products is increasing over time. Because no significant cracking was observed after the thermal treatment of quartzite without Solar Salt, it is assumed that the cracking is caused by the diffusion of the sodium and into the particles forming natrosilit or NaSiO phase. As a result of the diffusion process the mineral compartments (small crystallites in the crystallographic sense) expand which eventually leads to crack formation. After extracting the sample from Solar Salt the stone particles appeared physically very stable and the particle shape has not changed significantly. It is possible that the observed cracks are refilled by natrosilit which is also stable in Solar Salt at high temperatures.

The same investigations were performed for BaHu and BaRo. In Figure 12 the microstructures of the basalt BaRo without thermal treatment (a) and after the isothermal test with duration of 1.000 (b), 5.000 (c) and 10.000 h (d) are presented.

Published in; Solar Energy *171* (1) **2018**, 827-840

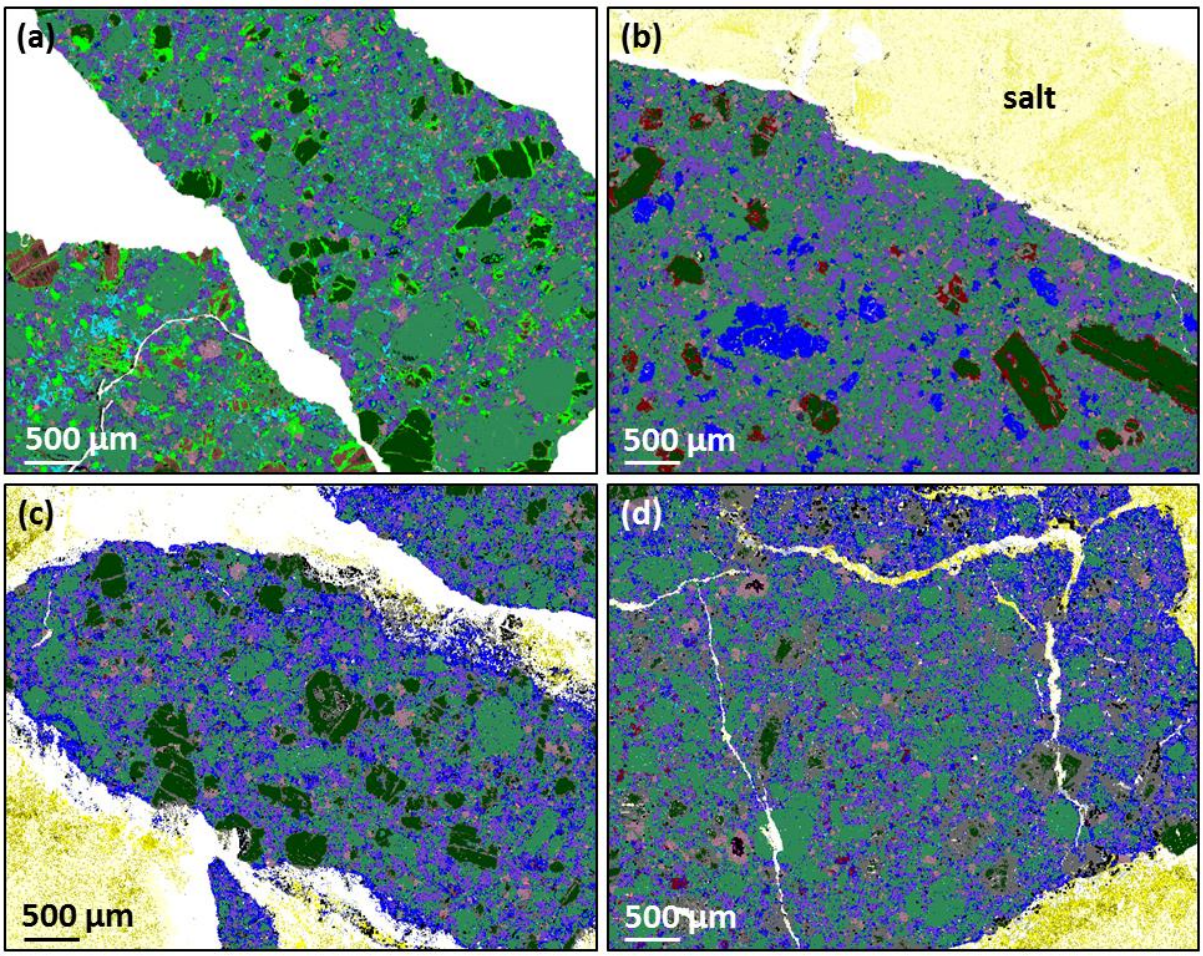

Figure 12 QEMSCAN images of BaRo particle(s) (a) prior to the experiments and (b) after 1.000h, (c) 5.000h, and (d) 10.000h of isothermal storage in Solar Salt.

After thermal treatment of the basalt BaRo the stone microstructure also changed. The main components, which increase with the duration of thermal treatment, are smectit-zeolith and layered silicates like biotite (brown areas) and altered biotite (dark grey areas). Smectit-zeolith, depicted as dark blue areas in Figure 12 b-d, and biotite formed at the particles-salt interface and also within the bulk of the particles. Simultaneously, the amounts plagioclase (torquise areas), clinopyroxene (grey green area) and nepheline (lilac area) phases decrease during the thermal treatment. In the long-term thermal treatment with 10.000 h cracking in the particle structure is detected.

After thermal treatment of BaHu similar changes in the particle structure are detected. The original composition mainly consists of clinopyroxene (green-grey), plagioclase (turquoise) and olivine (dark green) as shown in Figure 13 a.

Published in; Solar Energy *171* (1) **2018**, 827-840

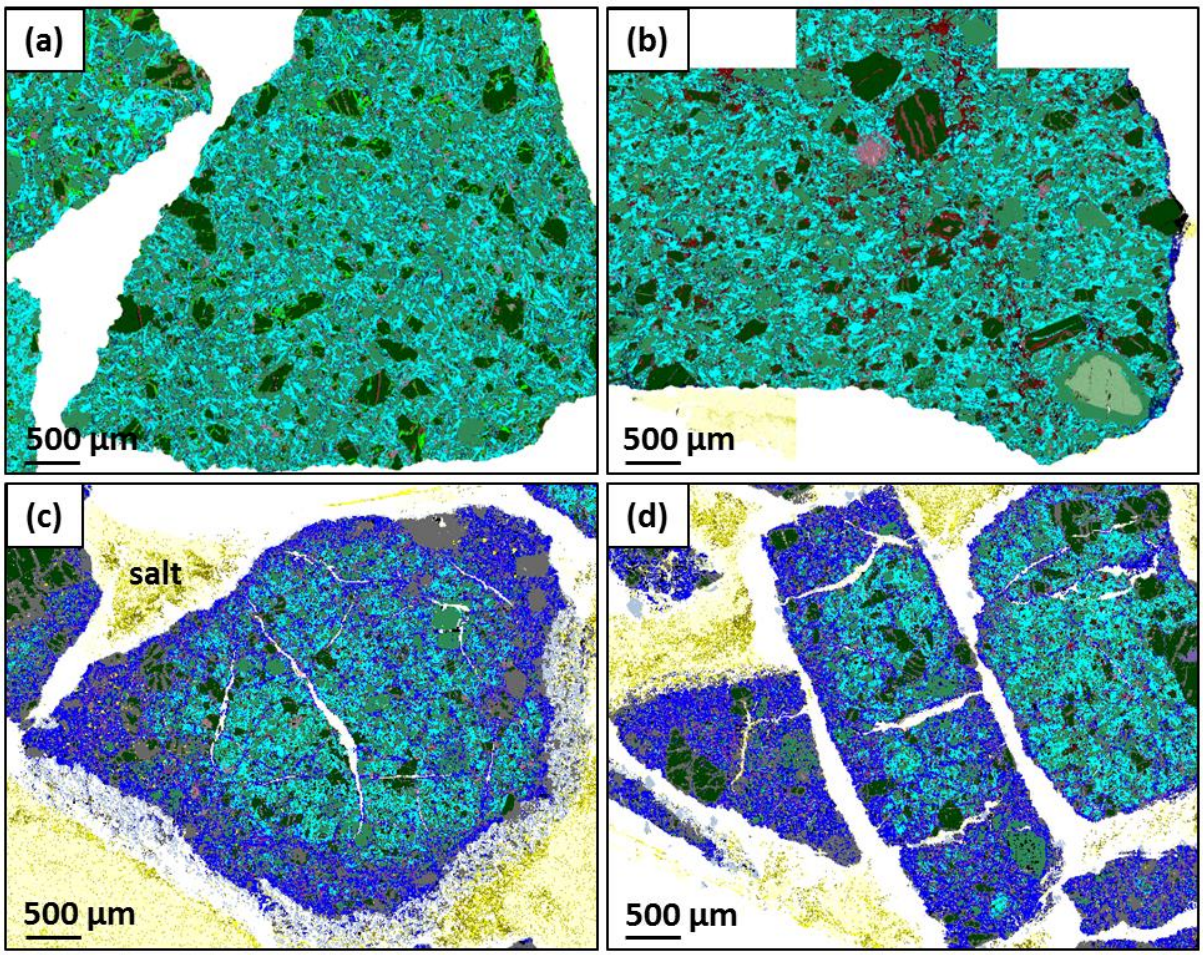

Figure 13 QEMSCAN images of BaHu particle(s) (a) prior to the experiments and (b) after 1.000h, (c) 5.000h, and (d) 10.000h of isothermal storage in Solar Salt.

After the thermal treatment in Solar Salt for 1.000 h the first changes in the microstructure can be detected (Figure 13 b), namely the transformation of olivine (dark green areas) into biotite (brown areas). With increasing duration of the isothermal treatment the olivine amount decreases with increasing biotite content. The second increasing stone component is smectit-zeolith. At the beginning, the smectit-zeolith is mainly detected along the particle-salt interface (Figure 13 b). After 5.000 h the share of smectit-zeolith in the composition increases strongly and this phase is detected within the bulk of the particle structure. The amount of the smectit-zeolith depending on duration of the isothermal test is shown in Figure 13 b-d. The progress of that genesis varied strongly among the different particles. Simultaneously, the amount of plagioclase and clinopyroxene beside olivine decreases in BaHu samples as mentioned before. After extracting the sample from Solar Salt at high temperatures, it was observed that the liquid salt is filled with dark small floating particles.
In addition to the isothermal tests, cyclic tests were performed as described by Martin et al. (2014) and the microstructure of the stones was analyzed.

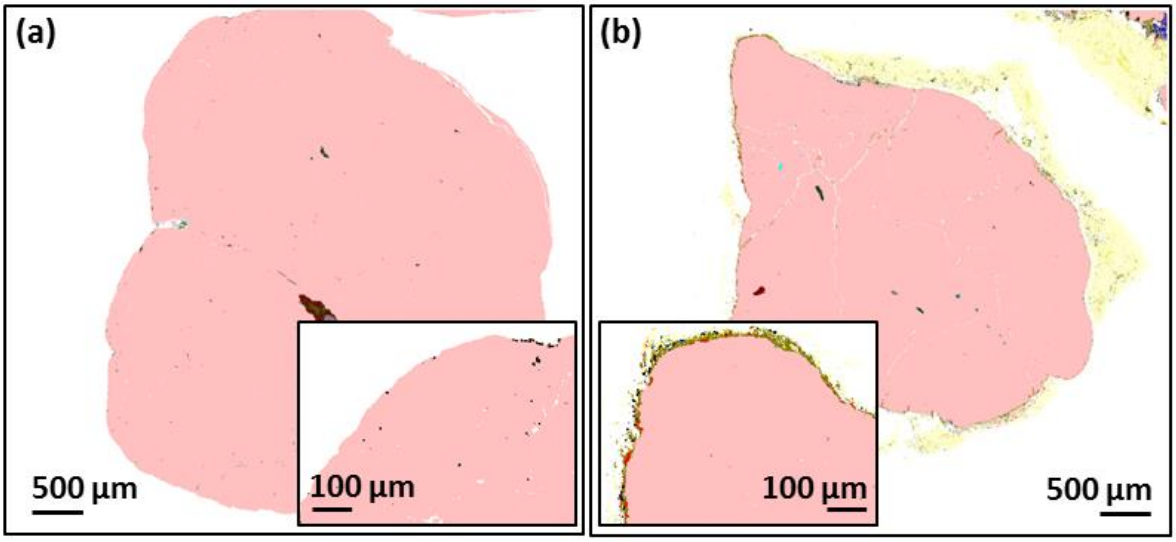

Figure 14 QEMSCAN images of quartz particles (a) before, and (b) after 100 cycles between 560°C and 290°C in Solar Salt.

As shown in Figure 14, the results are comparable with the isothermal test at high temperature up to 560 °C. Along the particle-molten salt interface natrosilit (red areas) is formed. The duration of the thermal treatment at high temperature level was 2 h per cycle so that the maximum duration at 560°C is only 200 h. With increasing number of cycles the formation of natrosilit will most likely increase.

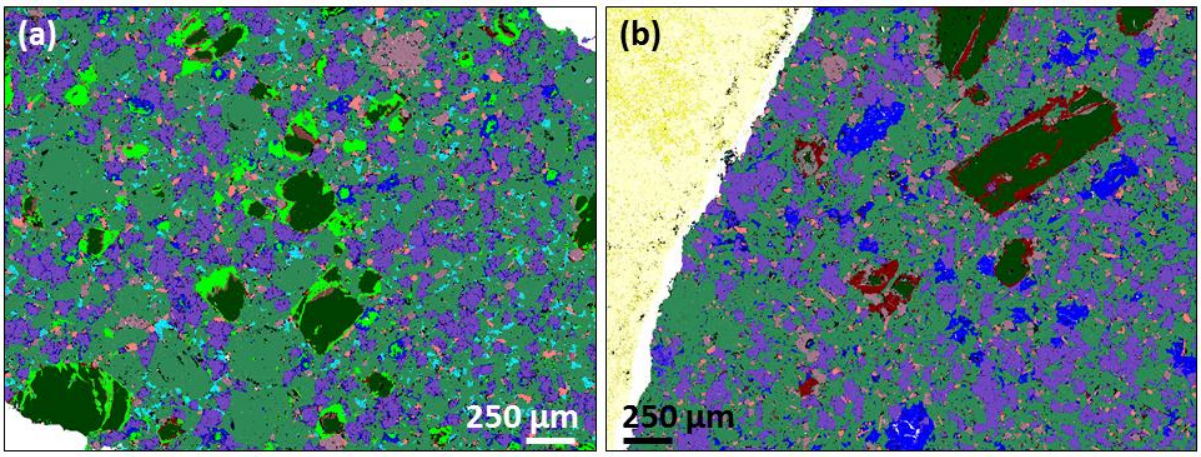

Figure 15 QEMSCAN image of BaRo (a) before, and (b) after thermal cycling in Solar Salt (100 cycles between 290 °C and 560 °C).

Figure 15 presents the particle structure before and after the cyclic thermal treatment of the basalt variety BaRo. The beginning formation of the two main components, smectit-zeolith (dark blue areas) and layered silicates like biotite (brown areas) are clearly visible. Components like plagioclase (torquise areas) and the silicate olivine (olive green areas) disappear during the thermal treatment. The results are also comparable with the isothermal test and due to the overall low duration at high temperatures the microstructures are comparable to those after 1.000h of isothermal storage.

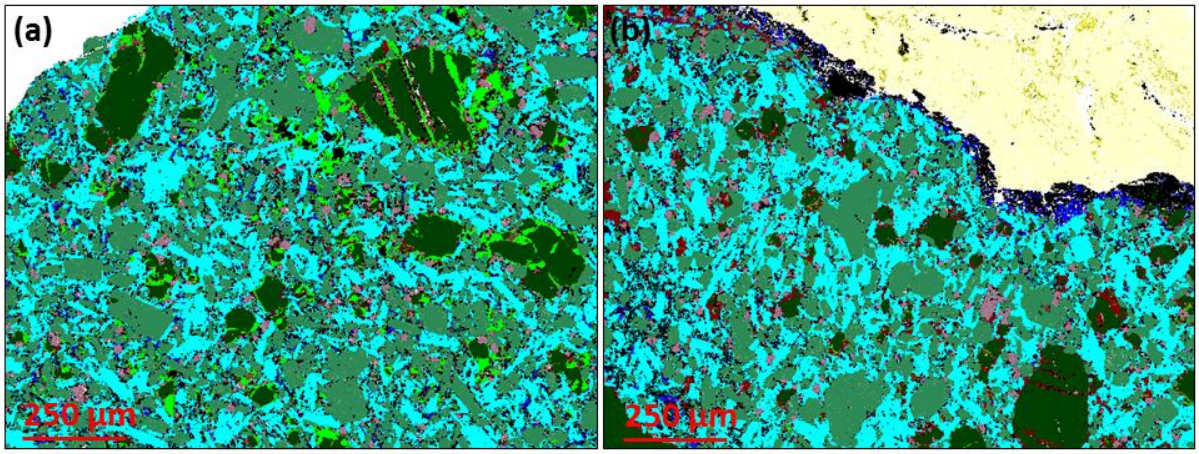

Figure 16 QEMSCAN image of BaHu (a) before, and (b) after thermal cycling in Solar Salt (100 cycles between 290°C and 560°C).

Figure 15 presents The particle structure before and after the cyclic thermal treatment of the basalt variety BaHu is presented in Figure 16. The change, due to the transformation from olivine (dark green areas) into biotite (brown areas) is not detected. However, the formation of smectit-zeolith is visible while the amount of plagioclase decreases. The observed change in the particle structure is comparable with the particles structure after the isothermal test for 1.000 h. It is assumed that the formation of smectit-zeolith increases with time and also the olivine-biotite transformation starts. The high amount of iron oxide is special for the investigated particle which was selected for QEMSCAN and is no result of the thermal treatment.

3.3. Solar Salt after thermal treatment

Besides the analysis of the natural stones before and after the thermal treatment the Solar Salt samples were investigated in particular their melting point and the salt composition. It is well accepted, that a nitrate/nitrite equilibrium establishes in nitrate salts at high temperatures (eq. (2)). Therein, the concentration of nitrite is directly related to the oxygen partial pressure of the gas atmosphere.

$$NO_3^- \rightleftharpoons NO_2^- + O_2 \qquad 2$$

This decomposition mechanism is commonly accepted and there is consensus, that equilibrium is achieved due to a naturally existing oxygen partial pressure over the system. However, further decomposition can occur, which has been postulated in the 80's (Nlssen, 1982). The species formed are typically oxides (hyperoxides, superoxides, peroxides or related species) which are formed by a reaction similar to that presented in eq. (3):

$$2NO_2^- \rightarrow O^{2-} + NO + NO_2 \qquad 3$$

While it is theoretically possible to push the back-reaction of (3), it is technically more likely that the formed nitrous gases are removed from the reaction since salts are typically stored in an open atmosphere or even a gas stream. Despite, the formed oxides are known to enhance corrosion of steel containers (Lovering, 1982) but can also further react with atmospheric carbon dioxide to form carbonates according to eq. (4):

$$CO_2 + O^{2-} \rightarrow CO_3^{2-} \qquad 4$$

On a relevant scale carbonate formation has been demonstrated in only a few cases where Solar Salt is stored in an open atmosphere (Bonk et al., 2017). Phase diagrams suggest that

precipitation occurs when carbonate concentrations in Solar Salt exceed 5 mol% (Amadori, 1913). However, related to filler materials in interaction with Solar Salt, not only atmospheric CO_2 may be a source of carbonate formation. Bonk et al. have demonstrated that carbonates in fillers ($CaCO_3$-phases or similar) can be leaked out of the filler compartments resulting in carbonate formation in the melt (Bonk et al., 2017).

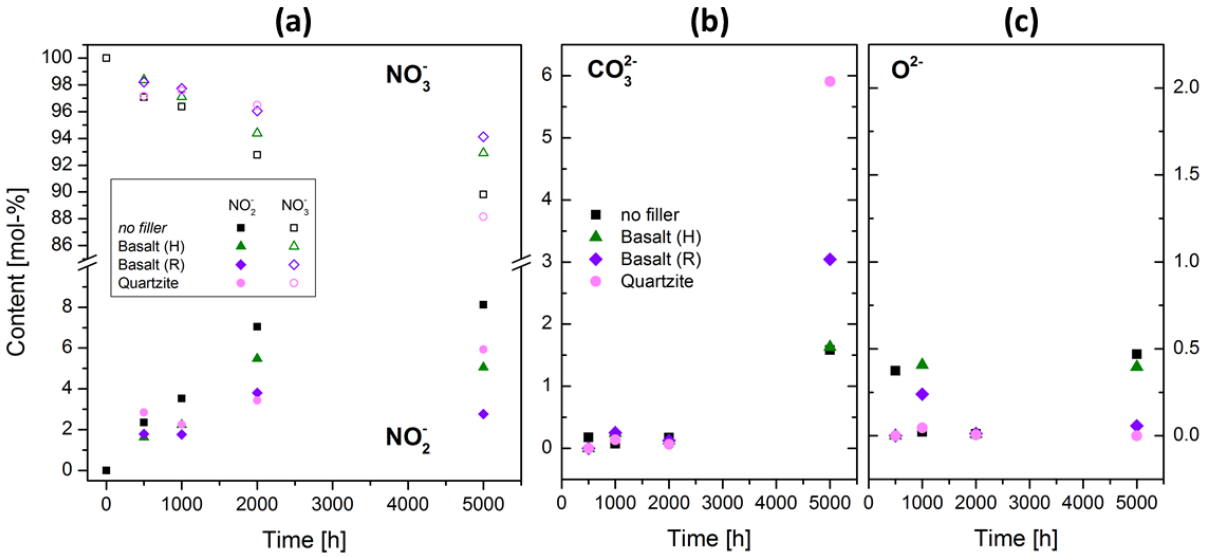

Figure 17 (a) nitrite and nitrate contents, (b) carbonate, and (c) oxide contents of Solar Salt stored with different filler particles as indicated. Legend presented in (b) also holds true for (c).

Figure 17 shows the nitrite, nitrate, carbonate and oxide contents in Solar Salt stored with the different filler materials over time. For all samples the nitrite content increases over time up to 5.000 h while the nitrate content decreases. This can be attributed to the steady decomposition of the nitrate ion to nitrite according to equilibrium reaction (3). It becomes obvious that interactions with the filler have no major effect on the nitrate/nitrite content. Therefore, it is neither diminished nor accelerated by the filler particles. Meanwhile, no significant oxide or carbonate formation can be detected up to 2.000 h. Interestingly, only after 5.000 h the carbonate content increases dramatically in Solar Salt stored with quartzite and only marginally for salts stored with the basalt types or without filler. In 10.000 h experiments, where no salt creeping and thus material loss was approbated, the carbonate and oxide contents (Table 4) are successively lower compared to those in 5.000 h experiments. We suggest that different storage conditions have a major influence on the stability of Solar Salt which has to be addressed in future work and exceeds the scope of this paper. As a short summary, the surface-to-volume ratio of the molten salt, the atmosphere and impurity types and levels can affect the molten salt stability. If for example product gases such as oxygen (eq. 2) or nitrous gases (eq. 3) are removed from the reaction zone (e.g. by flushing with N_2 or Ar atmosphere), the reaction equilibrium is shifted to the nitrite and oxide-side, in other words decomposition of the molten salt is promoted. Impurity effects are more complex. The most important impurities are magnesium, chlorides and oxides which enhance decomposition reaction rates and/or increase corrosiveness of the molten salt. Furthermore, the salt creeping observed in some of the experiments may have led to the concentration of oxide and carbonate species after prolonged storage times resulting in higher concentrations of those species in the finally extracted melt. More extensive investigations are required to elucidate this hypothesis.

Table 4 Anion contents in Solar Salt after isothermal storage with different filler materials for 10.000 h.

Filler type	Content [mol%]			
	NO_3^-	NO_2^-	CO_3^{2-}	O^{2-}
No filler	92.93	6.90	0.17	0.00
Quartz	95.54	4.14	0.32	0.00
BaHu	96.70	3.14	0.16	0.00
BaRo	95.70	4.17	0.12	0.01

The influence of changing salt chemistry on the thermal properties of Solar Salt was investigated by DSC methods. In previous thermal test, presented from Martin et al. (2014) deviations of the melting point before and after the thermal tests are in the range from 10 to 17 K. The deviation increases with the test duration. The melting onset and the melting enthalpy, which reflect changes in the salt chemistry, were measured and are plotted in Figure 18. It is observed that the melting enthalpy of the salt samples decreases over time for all samples. This may on the one hand be due to the increasing nitrite content as demonstrated by Bauer et al. (2012), while also cation exchange with the filler materials may have affected the melting enthalpy.

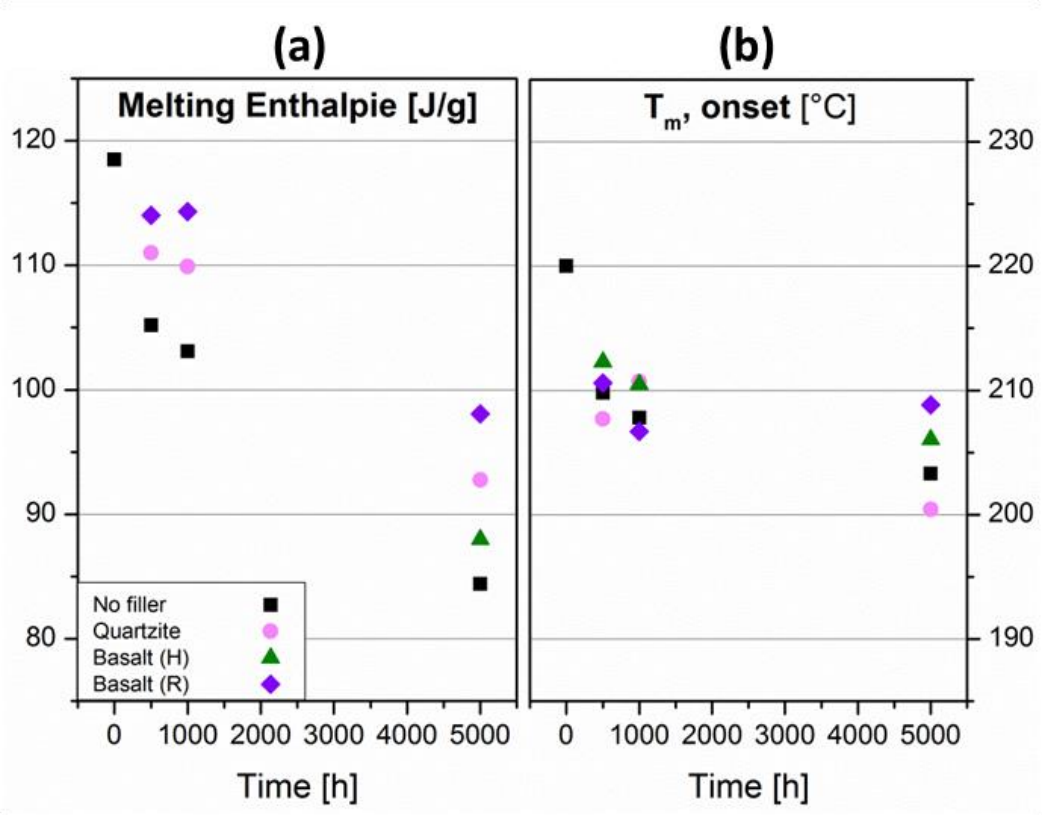

Published in; Solar Energy *171* (1) **2018**, 827-840

Figure 18 (a) melting enthalpies, and (b) melting onsets of Solar Salt stored with different filler particles as indicated. Data was reprinted from ref (Bonk et al., 2017)

Similar to the changes in the melting enthalpy the melting point itself is affected. It decreases over time which we attribute to the increasing nitrite content. The latter is known to affect the melting temperature (in this case the onset of melting) ultimately the reason for the development of binary reciprocal salt compositions such as Hitec (KNO_3-$NaNO_2$-$NaNO_3$). In this study, the melting temperatures decrease by up to 20 °C down to a melting onset of 200 °C.

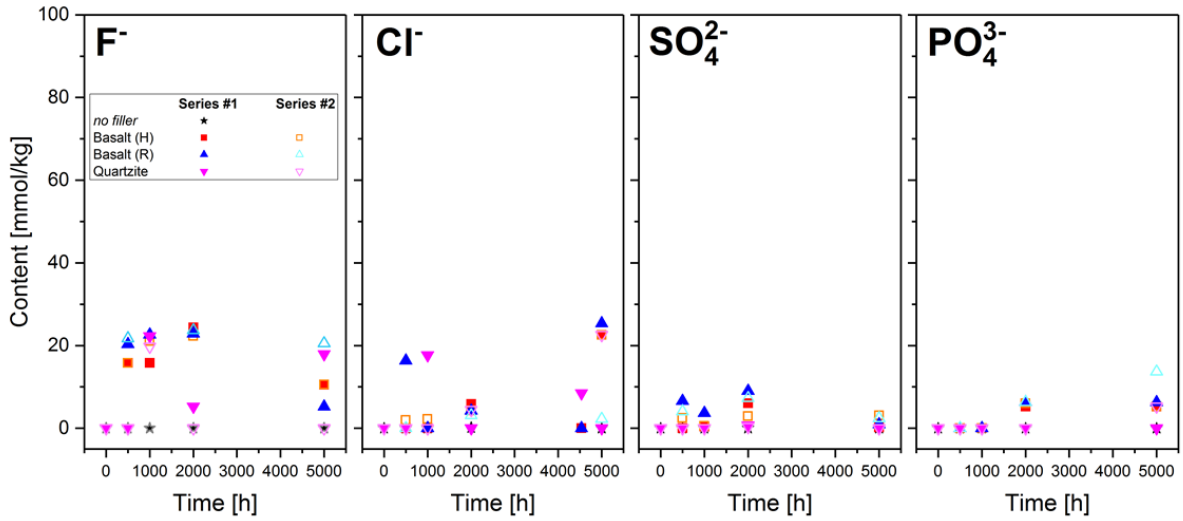

Figure 19 Different sub-contents of fluoride, chloride, sulphate and phosphate anions in Solar Salt, stored with filler materials, measured by ion chromatography

In addition to the presence of the four anions presented, traces of other anions namely, fluoride, chloride, sulfate and phosphate are detectable. Despite their detectable concentrations, presented in Figure 19, they present no concern to the designated technical process, since severe precipitation reactions are not to be expected.

4. Conclusions

This paper presents investigations on the stability of potential filler materials basalt and quartzite for operating temperatures up to 560 °C in Solar Salt utilizing a thermocline storage system. Long term isothermal storage experiments (up to 10.000 h) and subsequent investigations of the stone's microstructure as well as the Solar Salt after thermal treatment are presented.

Summarizing the material properties of quartzite and basalt, it can be noted that the specific heat capacity of quartzite is higher than that of basalt especially in the temperature range above 400 °C. Basalt exhibits higher maximum values for gross density and compressive strength. Both properties are important for potential filler materials whereby the specific heat capacity determined the storage capacity of the storage unit.

Isothermal tests at temperatures of 560 °C in air atmosphere show no significant changes in the stone structure of quartzite. At the basalt variety BaRo (strip mining *Rossdorf)* the share of nepheline ($NaAlSiO_4$) decrease while the smectit-zeolith are increase. During the thermal treatment of basalt BaHu (strip mining *Huehnerberg*) a reduction of clinopyroxene and an increasing of layered silicates were detected. Cracking was not observed by both basalt varieties. The measured mass losses are unobtrusive.

The focus of that study was the investigation of the stone composition after the isothermal test in Solar Salt with a maximum temperature of 560 °C. The stone components were investigated by using QEMSCAN, a combination of X-ray spectroscopy and scanning electron microscopy. The Solar Salt environment caused changes in the composition of both selected filler materials. The changes were quite varied. Significant differences among the examined filler materials with respect to the degradation mechanism were found. On the particle-molten salt interfaces of quartzite, mainly natrosilit ($Na_2Si_2O_5$) and a SiNaO phase are formed, where for basalt intragranular changes occurred. The arising components seem also to be stable at the operating temperature of 560 °C. The main transformation products of the basalt BaRo and BaHu are smectit-zeolith and biotite. Other components of the basalt disappear over the duration of the thermal treatment, namely plagioclase, olivine, clinochlore, chamosite, clinopyroxene and nepheline. In some Solar Salt samples extracted after the isothermal storage, dark particles are observed floating on the surface deriving from particle degradation of the basalt. The cyclic thermal test between 290 and 560 °C confirm the results of the isothermal test to the effect that similar decomposition products and microstructural changes in the filler materials are observed. In summary, it can be noted that quartzite, or principally SiO_2, continuously reacts with Na^+ to form natrosilit and SiNaO phase. The chemical compositions of the basalt varieties are more complex but also understandable in terms of reactions of molten salt with siliceous oxides. Overall, the observed cracking in the microstructure of basalts was less severe than in the quartzite particles. For using filler materials in Solar Salt further investigation concerning the long-time lifetime using isothermal test are required. It is recommended to monitor both, chemical and microstructural changes in the filler, as well as changes in the salt chemistry. Another aspect is the variation of filler composition depending on the mining location. Utilization of filler will require an understanding of these differences and their impact on the lifetime, as well as the development of filler monitoring and selection methods.

The measurements of the melting enthalpy and the melting point of the Solar Salt after the thermal treatment reveal that the both values decrease over the duration independent of the filler material. Overall, the salt chemistry is not severely affected by the interaction with quartzite, BaHu and BaRo as reflected by the results from ion chromatography and thermal analysis after molten salt tests without filler.

Acknowledgement

The authors thank the German Federal Ministry for the Environment, Nature Conservation and Nuclear Safety for the financial support given to the MS-Store project (Contract No. 0325497A).

Reference

Amadori, M., 1913. Atti reale. Atti Real. Acad. Lincei Sez. II 22, 366.

Bauer, T., Laing, D., Tamme, R., 2012. Characterization of sodium nitrate as phase change material. Int. J. Thermophys. 33, 91–104. doi:10.1007/s10765-011-1113-9

Bayón, R., Rojas, E., 2014. Analytical function describing the behaviour of a thermocline storage tank: A requirement for annual simulations of solar thermal power plants. Int. J. Heat Mass Transf. 68, 641–648. doi:10.1016/j.ijheatmasstransfer.2013.09.070

Bayón, R., Rojas, E., 2013. Simulation of thermocline storage for solar thermal power plants: From dimensionless results to prototypes and real-size tanks. Int. J. Heat Mass Transf. 60, 713–721. doi:10.1016/j.ijheatmasstransfer.2013.01.047

Bazant, Z.P., Kaplan, M.F., 1996. Concrete At High Temperatures: Material Properties and Mathematical Models. Longman, Harlow.
Biencinto, M., Bayón, R., Rojas, E., González, L., 2014. Simulation and assessment of operation strategies for solar thermal power plants with a thermocline storage tank. Sol. Energy 103, 456–472. doi:10.1016/j.solener.2014.02.037
Bonk, A., Martin, C., Braun, M., Bauer, T., 2017. Material investigations on the thermal stability of solar salt and potential filler materials for molten salt storage. AIP Conf. Proc. 1850, 80008. doi:10.1063/1.4984429
Brosseau, D.A., Hlava, P.F., Kelly, M.J., 2005. Testing Thermocline Filler Materials and Molten - Salt Heat Transfer Fluids for Thermal Energy Storage Systems Used in Parabolic Trough Solar Power Plants, Solar Energy Eng-Trans ASME. Albuquerque, New Mexico. doi:10.1115/ISEC2004-65144
Bruch, A., Fourmigué, J.F., Couturier, R., 2014. Experimental and numerical investigation of a pilot-scale thermal oil packed bed thermal storage system for CSP power plant. Sol. Energy 105, 116–125. doi:10.1016/j.solener.2014.03.019
Burolla, V.P., Bartel, J.J., 1979. High temperature compatibility of nitrate salts, granite rock and pelletized iron orem, SAND79-8634. Albuquerque, New Mexico.
Calvet, N., Gomez, J.C., Faik, A., Roddatis, V. V., Meffre, A., Glatzmaier, G.C., Doppiu, S., Py, X., 2013. Compatibility of a post-industrial ceramic with nitrate molten salts for use as filler material in a thermocline storage system. Appl. Energy 109, 387–393. doi:10.1016/j.apenergy.2012.12.078
Chang, Z., Li, X., Xu, C., Chang, C., Wang, Z., Zhang, Q., Liao, Z., Li, Q., 2016. The effect of the physical boundary conditions on the thermal performance of molten salt thermocline tank. Renew. Energy 96, 190–202. doi:10.1016/j.renene.2016.04.043
Cornell, R.M., Schwertmann, U., 2003. The Iron Oxides. Wiley-VCH Verlag GmbH & Co. KGaA, Weinheim, FRG. doi:10.1002/3527602097
DIN Deutsches Institut für Normung e.V., 2007. DIN 52100-2:2007-06 Natural Stones - Petrographic examinations - General and summary. Germany.
Fa. Dorfner GmbH, 2012. Product Data Sheet Quartzite.
Faas, S.E., Thorne, L.R., Fuchs, E.A. ; Gilbertsen, N.D., 1986. 10 MWe Solar Thermal Central Receiver Pilot Plant: Thermal Storage Subsystem Evaluation Final report. United States.
Flueckiger, S.M., Yang, Z., Garimella, S. V., 2013. Design of Molten-Salt Thermocline Tanks for Solar Thermal Energy Storage. Heat Transf. Eng. doi:10.1080/01457632.2012.746152
Gaggioli, W., Fabrizi, F., Tarquini, P., Rinaldi, L., 2015. Experimental validation of the innovative thermal energy storage based on an integrated system " storage tank / steam generator ." Energy Procedia 69, 822–831. doi:10.1016/j.egypro.2015.03.091
Gil, A., Medrano, M., Martorell, I., Lázaro, A., Dolado, P., Zalba, B., Cabeza, L.F., 2010. State of the art on high temperature thermal energy storage for power generation. Part 1—Concepts, materials and modellization. Renew. Sustain. Energy Rev. 14, 31–55. doi:10.1016/j.rser.2009.07.035
González, I., Lehmkuhl, O., Pérez-Segarra, C.D., Oliva, A., 2015. Dynamic Thermoelastic Analysis of Thermocline-like Storage Tanks. Energy Procedia 69, 850–859. doi:10.1016/j.egypro.2015.03.106
Grirate, H., Agalit, H., Zari, N., Elmchaouri, A., Molina, S., Couturier, R., 2016. Experimental and numerical investigation of potential filler materials for thermal oil thermocline storage. Sol. Energy 131, 260–274. doi:10.1016/j.solener.2016.02.035
Grirate, H., Zari, N., Elmchaouri, A., Belcadi, S., Couturier, R., 2014. Physico-chemical and thermal analyzes of rocks used as filler material for thermal energy storage in CSP power plants. Energy Procedia 49, 810–819. doi:10.1016/j.egypro.2014.03.088
Grosu, Y., Faik, A., Ortega-Fernández, I., D'Aguanno, B., 2017. Natural Magnetite for thermal energy storage: Excellent thermophysical properties, reversible latent heat transition and controlled thermal conductivity. Sol. Energy Mater. Sol. Cells 161, 170–176. doi:10.1016/j.solmat.2016.12.006
Hoffmann, J.-F., Fasquelle, T., Goetz, V., Py, X., 2016. A thermocline thermal energy storage

system with filler materials for concentrated solar power plants: Experimental data and numerical model sensitivity to different experimental tank scales. Appl. Therm. Eng. 100, 753–761. doi:10.1016/j.applthermaleng.2016.01.110
John, E., Hale, M., Selvam, P., 2013. ScienceDirect Concrete as a thermal energy storage medium for thermocline solar energy storage systems. Sol. Energy 96, 194–204. doi:10.1016/j.solener.2013.06.033
Kolb, G.J., 2011. Evaluation of Annual Performance of 2-Tank and Thermocline Thermal Storage Systems for Trough Plants. J. Sol. Energy Eng. 133, 31023. doi:10.1115/1.4004239
Kolb, G.J., Lee, G., Mijatovic, P., Emanull, V., 2011. Thermal Ratcheting Analysis of Advanced Thermocline Energy Storage Tanks, in: SolarPaces 2011. United States.
Libby, C.S., 2010. Solar Thermocline Storage Systems: Preliminary Design Study. doi:Report no. 1019581, EPRI, California
Lovering, D.G., 1982. Molten Salt Technology. Springer US. doi:10.1007/978-1-4757-1724-2
Martin, C., Breidenbach, N., Eck, M., 2014. Screening and Analysis of Potential Filler Materials for Molten Salt Thermocline Storages. Proc. ASME 2014 8th Int. Conf. Energy Sustain. doi:10.1115/ES2014-6493
Nlssen, D.A., 1982. Literature Cited Thermophysical Properties of the Equimolar Mixture NaN0,-KNO, from 300 to 600 "C. J. Chem. Eng. Date 27, 269–273. doi:10.1021/je00029e012
Odenthal, C., Klasing, F., Bauer, T., 2017. Demonstrating Cost Effective Thermal Energy Storage in Molten Salts: : DLR's TESIS Test Facility. Energy Procedia 135, 14–22. doi:10.1016/j.egypro.2017.09.483
Ortega-Fernández, I., Calvet, N., Gil, A., Rodríguez-Aseguinolaza, J., Faik, A., D'Aguanno, B., 2015. Thermophysical characterization of a by-product from the steel industry to be used as a sustainable and low-cost thermal energy storage material. Energy 89, 601–609. doi:10.1016/j.energy.2015.05.153
Pacheco, J.E., Showalter, S.K., Kolb, W.J., 2002. Development of a Molten-Salt Thermocline Thermal Storage System for Parabolic Trough Plants. J. Sol. Energy Eng. 124, 153. doi:10.1115/1.1464123
Riaz, M., Minnesota., U. of, States., U., Administration., E.R. and D., Systems., D. of E.S., States., U., Energy., D. of, Systems., D. of E.S., 1977. Rock bed heat accumulators. Dept. of Energy, Division of Energy Storage Systems ; For sale by the National Technical Information Service, [Washington]; Springfield, Va.
Rodat, S., Bruch, A., Dupassieux, N., Mourchid, N. El, 2015. Unique Fresnel Demonstrator Including ORC and Thermocline Direct Thermal Storage: Operating Experience. Energy Procedia 69, 1667–1675. doi:10.1016/j.egypro.2015.03.127
Sassine, N., Donzé, F.-V., Bruch, A., Harthong, B., 2016. Rock-Bed Thermocline Storage: A Numerical Analysis of Granular Bed Behavior and Interaction with Storage Tank, in: Solar Paces 2016.
Smykatz-Kloss, W., 1970. Die Hoch-Tiefquarz-Inversion als petrologisches Hilfsmittel. Contrib. to Mineral. Petrol. 26, 20–41. doi:10.1007/BF00373338
Votyakov, E. V., Bonanos, A.M., 2015. Algebraic model for thermocline thermal storage tank with filler material. Sol. Energy 122, 1154–1157. doi:10.1016/j.solener.2015.10.047
Williamson, J., Glasser, F.P., 1965. Phase Relations in the System Na2Si2O5-SiO2. Science (80-.). 148, 1589 LP-1591.